

Chapter 11

Tracking of Backbone Curves of Nonlinear Systems Using Phase-Locked-Loops

Simon Peter, Robin Riethmüller, and Remco I. Leine

Abstract In nonlinear systems the resonance frequency depends on the energy in the system. This change in resonance frequency contains valuable information about the systems behavior and the nonlinear normal modes (NNMs) associated with each point of the backbone curve. This information can e.g. be used for system identification. However, the accurate and efficient measurement of the backbone curve in nonlinear systems is still challenging. This contribution proposes a new method to measure the backbone curve which is based on the control concept of a Phase-Locked-Loop (PLL) which is well known in electronics applications. A properly designed PLL is capable of finding linear resonances but it can also be used for the tracking of energy dependent backbone curves. The new method provides very accurate results by using steady state responses in the nonlinear mode. In contrast to commonly used free decay measurements this approach eliminates transient effects. Yet, it is also very efficient and user friendly as an automated testing can be performed. The method is experimentally demonstrated on a beam structure with cubic nonlinearity. Furthermore the capability of tracking through internal resonant NNMs will be examined and new possibilities for quantitative measurements of these effects will be discussed.

Keywords Phase-locked-loop • Nonlinear normal modes • Nonlinear system identification

11.1 Introduction

For the identification of linear vibrating systems experimental modal analysis (EMA) is the standard procedure, not only because it provides extensive information about the system in a very condensed form, but also because it is a very fast and user friendly procedure. In recent years an increasing number of researchers have worked on developing an extension of modal analysis to nonlinear systems. Starting with the theoretical developments of Rosenberg [1], the concept of Nonlinear Normal Modes (NNMs) emerged as a promising approach within this development. Rosenberg's definition of NNMs as the synchronous periodic motion of a conservative system provides interesting insights into the nonlinear dynamics of conservative systems and provides a clear relation to linear modes. Extending the concept of nonlinear modes, Shaw and Pierre [2] proposed the invariant manifold approach showing that a motion of a dynamic system in a nonlinear mode can be described as a motion on a two dimensional manifold. However, for complex structures and experimental approaches the invariant manifold approach poses practical difficulties and many systems can be characterized based on the dynamics of an underlying conservative system. Hence, most research in the area of nonlinear modal analysis relies basically on Rosenberg's definition [3]. A slight change of this definition was proposed by Kerschen [4] explicitly including internal resonances by dropping the requirement of a synchronous motion. Numerous publications have shown the usefulness of this concept for understanding nonlinear dynamics even of complex structures like for example aerospace engineering [5, 6]. It also provides a clear relation to linear modes and can also be related to forced response analysis of damped systems [7, 8]. On the one hand reliable numerical algorithms such as shooting [9] and the Harmonic Balance Method (HBM) [10] have been proposed and on the other hand some effort has been made in experimentally determining NNMs. The first approach of experimentally determining the nonlinear modes of lightly damped structures was the phase resonance method proposed by Peeters [11]. For determining the NNMs a system is driven to resonance at a high excitation level, then the excitation is turned off and a time frequency analysis of the free decay is carried out. This method proved its robustness and accuracy in experimental applications [12, 13] and can still be regarded as the standard method for nonlinear modal testing. Even though more recently a phase separation concept has been proposed [14] the phase resonance approach remains an important basis for nonlinear modal analysis. However, there are some practical issues arising from this procedure. The tuning of the

S. Peter (✉) • R. Riethmüller • R.I. Leine
Institute for Nonlinear Mechanics, University of Stuttgart, Pfaffenwaldring 9, 70550 Stuttgart, Germany
e-mail: peter@inn.uni-stuttgart.de

excitation is troublesome especially in the case of strong nonlinearity where a jump in the Frequency Response Function (FRF) occurs. Close to resonance, even for small disturbances, the jump can occur prematurely. Also the tuning, which is usually done manually, is time consuming and the estimation of an excitation level driving the system in a nonlinear range requires some a priori knowledge about the system or several trial and error runs. Additionally, by using the time frequency analysis of a free decay, sophisticated signal processing such as wavelet transforms [15] is required and some inaccuracy might be induced due to transient effects.

This paper presents a novel method for phase resonance testing to overcome these practical issues by an automated procedure using a PLL. The PLL is originally an analogue circuit used in radio technology in the 1930s [16] and is nowadays widely used in electronics applications like radios, TVs or smart phones [17]. The general idea of PLL concepts is to generate a harmonic signal with a frequency which is tuned based on the phase difference to a reference signal. There are many different designs of PLLs which are all essentially nonlinear oscillators generating a harmonic output dependent on this phase difference. The design of the PLL has to be adapted to its application which can be the tuning of digital or analogue signals originating from linear or nonlinear systems [18, 19]. Yet, only few attempts have been made to use these concepts for the measurement of mechanical structures. Most of them remain theoretical and the examples are mostly numerical ones [20]. There have been attempts to use PLLs in nonlinear micro systems modeled with one DOF [21] but the applicability for testing macro scale mechanical systems or continuous structures is mostly unclear. A publication by Mojrzisch [22] showed the usefulness of the PLL experimentally for the measurement of nonlinear FRFs of a macro scale single DOF Duffing type system by phase sweeping. However, to the authors knowledge there have no attempts been made to use the PLL for tracking of backbone curves of nonlinear continuous structures and exploit its potential for the measurement of NNMs.

The paper is organized as follows. In Sect. 11.2 some basics of phase resonance testing for nonlinear structures are briefly reviewed. In the subsequent Sect. 11.3 some more specific aspects of phase resonance method using the PLL including some design aspects of the PLL used within this paper are explained. In Sect. 11.4 a numerical example is used to illustrate the method and highlight some of its characteristics. The numerical example is followed by an experimental demonstration of its functionality in Sect. 11.5. The paper closes with a conclusion and some aspects of future work in Sect. 11.6.

11.2 Nonlinear Modal Analysis Using the Phase Resonance Method

A general mechanical system with conservative nonlinearities can be described in a spatially discretized form by the differential equation

$$M\ddot{x} + D\dot{x} + Kx + F_{nl}(x) = F_{exc}(t), \quad (11.1)$$

where M denotes the mass matrix, D the viscous damping matrix, K the linear stiffness matrix and $F_{nl}(x)$ represents a vector of nonlinear, conservative forces. The vector of external excitation is represented F_{exc} . In contrast, the NNMs of an autonomous conservative system are governed by a differential equation of the form

$$M\ddot{x} + Kx + F_{nl}(x) = 0. \quad (11.2)$$

For numerical systems periodic solutions of this differential equation can be obtained in a straightforward way using shooting or the HBM. These periodic solutions provide the NNMs of the system and can for example be visualized in Frequency Energy Plots (FEPs) [4]. Due to its high efficiency and its filtering property, which is particularly interesting in conjunction with measurements, the numerical NNM calculations throughout this paper are obtained by the HBM. The details of the numerical method are described in a previous publication [23]. The experimental realization of periodic motions of systems which motions are governed by differential Eq. (11.2) is more difficult as undamped systems cannot be realized practically as there are always sources of material damping or damping in interfaces of coupled structures. Hence, the forced and damped system described by Eq. (11.1) has to be considered as a representation of real systems. For lightly damped structures the assumption of proportional damping can provide a reasonable approximation. For the realization of a NNM motion of the underlying conservative system, the non-conservative system is sought to behave like a system described by Eq. (11.2). By comparing Eqs. (11.2) and (11.1) it can be seen that theoretically the forcing should exactly balance out the damping for all points of the structure and for all times i.e.

$$D\dot{x}(t) = F_{exc}(t), \forall t. \quad (11.3)$$

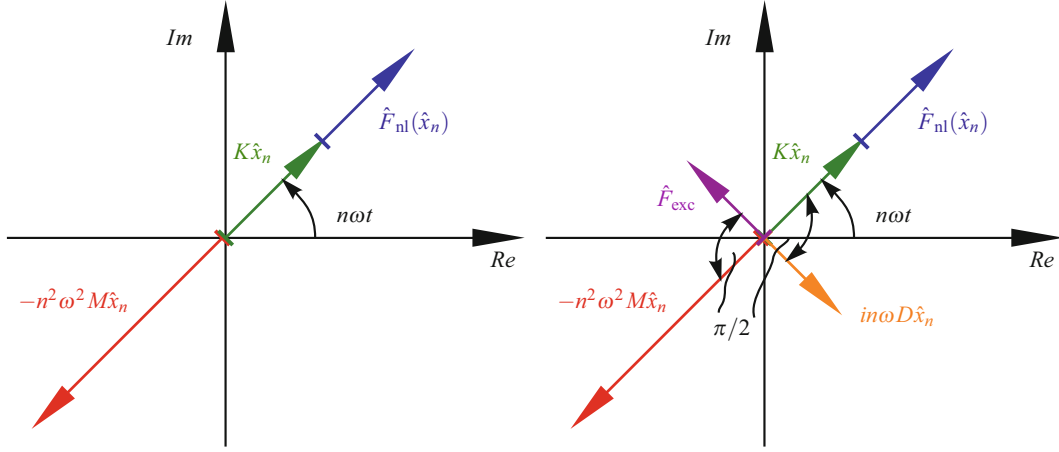


Fig. 11.1 *Left:* Pointer diagram for the n -th harmonic of a steady state NNM motion. *Right:* Pointer diagram for the n -th harmonic of a steady state NNM motion in a forced and damped system

For the realization of this state Peeters [11] derived a nonlinear mode indicator function similar to the mode indicator functions used in linear EMA. The derivation can be done by developing the displacements into an infinite cosine series and practically regarding the system's motion in the frequency domain. Similarly, the same mode indicator function can also be derived graphically using pointer diagrams. The application of pointers as a graphical representation of a signal is more common in electrical engineering but was also used e.g. in [24] in the context of multi-harmonic excitation of linear mechanical systems. As the NNMs represent a periodic motion of all DOFs, they can be transformed into the frequency domain using an infinite Fourier transform. Hence, the motion of the system can be represented by a fundamental frequency ω plus an infinite number of higher harmonics. For every harmonic the dynamic force equilibrium yielding the periodic motion can then be graphically represented as a family of pointers in the complex plane. To obtain a periodic motion the dynamic forces have to balance out for every harmonic. In Fig. 11.1 on the left this dynamic force equilibrium for the n -th harmonic is depicted symbolically for an autonomous conservative system. If this equilibrium condition is fulfilled for every harmonic, the system moves in a periodic NNM motion. This approach can be also viewed as a graphical representation of the HBM on a signal processing level. The same condition holds for a forced and damped system executing a steady state motion, simply adding two more pointers, namely the pointer of the n -th harmonic excitation force and damping force. It can be clearly seen that the pointer of the damping forces must be fully compensated by the pointer of the excitation forces, to ensure the NNM motion which is depicted in the left pointer diagram. As in the case of viscous damping, the damping force has a phase lag of $\pi/2$ with respect to the conservative restoring forces, or the displacement respectively. This means that the phase lag between the excitation force F_{exc} and the displacement must be $\pi/2$ for every harmonic n to generate an NNM motion.

Practically, the exact phase condition is impossible to maintain as it implies a fully populated forcing vector \hat{F}_{exc} with higher harmonic amplitudes and phases that have to be adjusted dynamically for every point on an NNM branch. This issue was addressed in several publication [8, 11, 12] and it was shown that a single harmonic forcing mostly provides a sufficient approximation for the NNM measurement in the case of light damping. This behavior can be explained as in most systems the majority of the NNM motions are governed by the fundamental harmonic and also the NNM frequency can in most cases be estimated accurately by a single harmonic approximation. However, especially near internal resonances the higher harmonics are amplified by higher modes and have significant influence on the systems motion. In this case the appropriate forcing has to be regarded more closely. In the following, a single harmonic force at a single point of the structure will be used to realize an approximate appropriate excitation. Some issues related to the accuracy of this approach and the presence of internal resonances are addressed in the numerical study in Sect. 11.4.

11.3 Phase Resonance Testing Using the Phase-Locked-Loop

Based on the phase criterion, derived in the previous section the NNM motion of a system can be approximately excited by an appropriate harmonic forcing with a phase lag of $\pi/2$ with respect to the response. In previous publications the tuning of the phase was done manually comparing the phase of the excitation with the phase of the response. This task can be

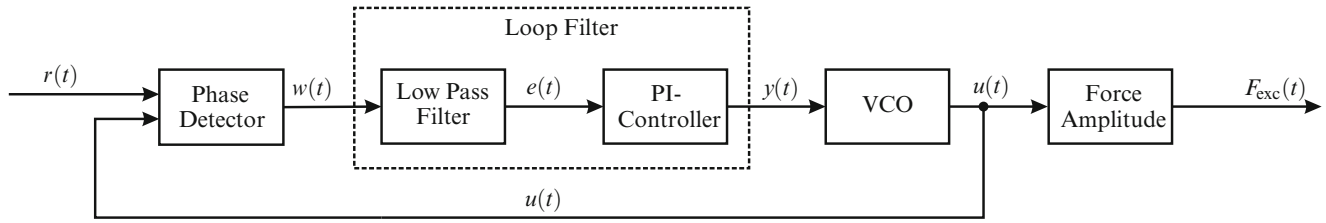


Fig. 11.2 Schematic structure of the PLL for force generation

automated by the use of a PLL which is a concept for the control of the phase between a reference and a harmonic output signal. There are different implementations of the PLL for different applications such as digital or analogue PLLs. Both versions of PLLs can be implemented electronically e.g. using Simulink. In the following, the design of an analogue PLL, which was implemented for the tuning of the phase in the context of NNM testing, is briefly described.

For this purpose a reference signal $r(t)$ of the system has to be connected to the PLL. The PLL synchronizes the phase of its output with this reference signal except for a desired phase difference. The reference signal can for instance be chosen based on the displacement of a reference point which then means that the phase difference of the output signal should be $\pi/2$. The equations for the PLL controller are derived in the following for this specific case. In an experimental setup it is reasonable to choose a reference signal based on the quantity that can directly be measured. Since in the experiments in Sect. 11.5 accelerometers are used, the reference signals in the experiments are based on the system's acceleration and the phase difference is set to $-\pi/2$. This can be achieved by simply multiplying the reference signal with a factor of -1 compared to the case of the displacement based measurements. Generally, a PLL used for the excitation of a structure consists of the blocks displayed schematically in Fig. 11.2.

The first block is the phase detector that extracts the phase of the output of the system with respect to the reference signal. There are different implementations of phase detectors [18]. In the following a mixing phase detector is used which is comparing a reference signal $r(t)$ with the output of the VCO $u(t)$ by a multiplication yielding

$$w(t) = r(t)u(t). \quad (11.4)$$

For the nonlinear modal analysis as a reference signal the displacement $x(t)$, velocity $\dot{x}(t)$ or acceleration $\ddot{x}(t)$ can directly be used depending on which quantity is measured. However, as was shown by Fan [20] it is advantageous to modify the signal of for instance the displacement by replacing it with its sign

$$r(t) = \text{sign}(x(t)) = \begin{cases} -1 & x(t) < 0 \\ 1 & x(t) \geq 0. \end{cases} \quad (11.5)$$

This modification leads to a faster and more robust PLL, as on the one hand the signal is amplified in regions which are far from resonance. On the other hand the stability criterion for the controller derived in [20] becomes independent of the forcing amplitude. For the phase detector both signals are expressed in form of Fourier series and their product can be written as

$$w(t) = \hat{r} \sin(\omega_r t + \phi_r) \cos(\omega_v t + \phi_v) + \text{higher order terms (HOT)}, \quad (11.6)$$

where ω_r and ω_v denote the frequency and ϕ_r and ϕ_v the phase of the fundamental frequency of the reference signal and the VCO respectively. It should be noted that the fundamental of the reference signal is generally different to the fundamental harmonic of the displacement or acceleration, respectively. This holds especially for the amplitude providing previously mentioned advantages. However, it should also be kept in mind that, if there is a phase shift between the fundamental harmonic and higher harmonics, there can also be a slight shift in the sign function in Eq. (11.4) and the phase of its fundamental harmonic. This effect will be illustrated in the numerical example in Sect. 11.4. After some trigonometric manipulations of Eq. (11.6) and the assumption that the frequency error is small $\omega_r \approx \omega_v \approx \omega$ the output of the phase detector can be expressed as a function of the phase error $\theta_e = \phi_v - \phi_r$ and higher frequency terms

$$w(t) = \frac{1}{2} \hat{r} (\sin(\theta_e) + \sin(2\omega t + \phi_v + \phi_r)) + \text{HOT}. \quad (11.7)$$

The output of the phase detector is passed to the second part of the PLL, which is the loop filter consisting of a low pass filter and a PI-controller. The low pass filter that can be described by the differential equation

$$\omega_l \dot{e} + e = w(t), \quad (11.8)$$

with the cutoff frequency ω_l . This means that the output of the low pass filter is a function of the phase error θ_e if the higher frequency terms in Eq. (11.7) are suppressed sufficiently. The output of the low pass filter is the control input of the PI-controller that can be described by the state space model

$$\begin{aligned} \dot{z} &= e \\ y &= K_p e + \frac{K_p}{T_i} z. \end{aligned} \quad (11.9)$$

The parameters K_p and T_i are the tuning parameters of the proportional and integral part of the controller. The exact tuning of these parameters is rather uncritical in the PLL as long as the stable low pass property of the PI-controller is retained. The PI-controller provides the control signal for the third part of the PLL, namely the Voltage-Controlled-Oscillator (VCO), that generates the excitation signal for the structure. The VCO uses the fact that the frequency is the derivative of the phase, and hence can be realized as an integrator

$$\theta_v = \int_0^t \omega_c + K_v y(\tau) d\tau, \quad (11.10)$$

with the center frequency ω_c and tuning parameter K_v . The center frequency ω_c is the frequency with which the VCO oscillates when no reference signal is attached and the tuning factor K_v adjusts the influence of the control input coming from the loop filter. Hence, the cosine output of the VCO is generated

$$u(t) = \cos(\theta_v). \quad (11.11)$$

This output signal is then fed back to the phase detector and the phase difference is minimized until the VCO creates a cosine signal with the same phase as the reference signal. Once this is the case the PLL is said to be in a locked state. The output of the VCO is multiplied by the excitation amplitude yielding

$$F_{\text{exc}}(t) = \hat{F}_{\text{exc}} u(t). \quad (11.12)$$

This force signal is then used for the excitation of the structure i.e. the created cosine shaped force signal is shifted by an angle of $\pi/2$ with respect to the sinusoidal reference signal in Eq. (11.6).

For a more detailed discussion of the design of PLLs there are numerous references [17, 18, 25]. Regarding the stability properties of the PLL, criteria can be derived using linear analysis methods like the Routh-Hurwitz criterion [20, 26] and nonlinear analysis methods like Lyapunov functions and La Salle's theorem [27]. It should be noted at this point that parameters can be found for this specific design of the PLL that ensure the stability of the PLL controller independent of the parameters of the attached system [27], which is essential when the PLL is used for the measurement of unknown structures.

With the PLL the backbone curve of a system can be measured in an automated two step methodology. In the first step the linear resonance is detected with low level excitation. Once the PLL is in a locked state the forcing level is incrementally increased such that the energy in the system increases. In nonlinear systems the resonance frequency changes with increasing energy and the PLL has to adjust the frequency of the VCO output with increasing energy to maintain the phase resonance criterion. The steady state vibration in resonance can be analyzed e.g. with an FFT or wavelet transform to extract the frequency amplitude dependence of the system. The use of the PLL for the measurement of NNM branches has several consequences compared to classical phase resonance testing:

1. There is no need for manual tuning of the phase as the PLL tunes the VCO and therefore the frequency of the excitation signal automatically.
2. The forcing is increased from a low to a high level in resonance until a desired level of vibration is reached such that the linear and nonlinear range is covered but the structure is not damaged. No a priori knowledge about nonlinear range or maximum forcing amplitude is required.

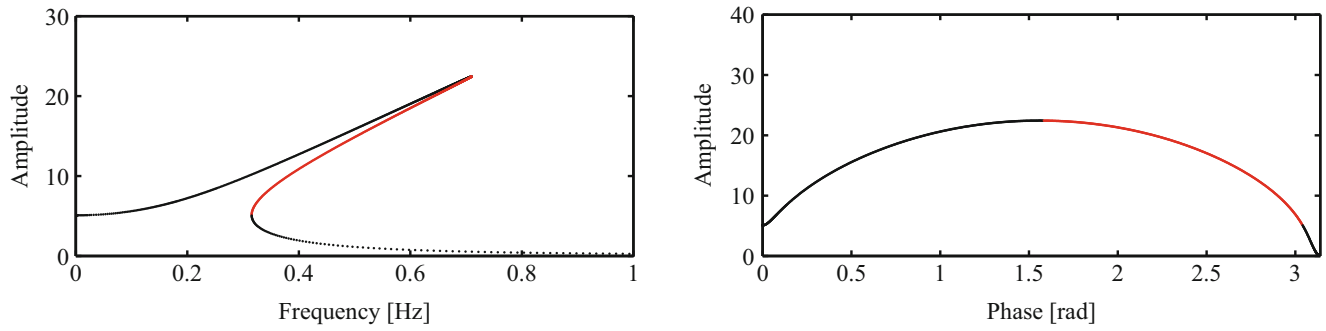


Fig. 11.3 FRF (*left*) and phase-amplitude-relation (*right*) for Duffing type example system (*black*: stable solutions, *red*: unstable solutions)

3. All measurements are carried out in steady state. No transient effects are present and signals can be analyzed with a simple FFT.
4. For low level excitation the linear resonance frequency is found and higher harmonics are negligible during resonance detection. Depending on the center frequency the VCO will lock to the corresponding mode.
5. In the nonlinear range small changes in excitation result in small changes of resonance frequency. Thus, the PLL reaches the locked state very fast and safely after increasing the excitation amplitude.
6. The PLL stabilizes unstable branches of the system such that premature jumps during the tuning in highly nonlinear systems are avoided. Because the control is based on the phase and the phase-amplitude relation is unique in the neighborhood of a mode as depicted in Fig. 11.3 all points of the phase-amplitude plane can be measured applying phase control [22].

These features will be illustrated in the following section by numerical examples before the method is applied to an experimental benchmark.

11.4 Parametric Study of a Numerical Example System

In this section the characteristics of the nonlinear modal test using the PLL are illustrated by a numerical example. Therefore, a beam structure similar to the ECL benchmark beam [28] is used as an example system. As illustrated in Fig. 11.4 the system consists of seven linear Euler-Bernoulli beam elements and has in total 14 DOFs. The beam is clamped on the left-hand side and is supported by a cubic and linear spring on the right-hand side. The system is excited at the second node and its parameters are listed in Table 11.1.

In the following mainly the first two NNMs of the system are considered which originate from the linear eigenfrequencies at 22.4 and 121.1 Hz respectively. Both of these modes are affected by the nonlinearity as it can be seen in the frequency energy plot (FEP) in Fig. 11.5. The FEP was calculated using the HBM taking into account three harmonics which is sufficient to represent a 1:3 internal resonance, which is the only internal resonance practically playing a role in the energy range of interest.

For the tests with the PLL the damped and forced system has to be regarded. The damping in the system is assumed to be light and the hypothesis of proportional damping of the form

$$\mathbf{D} = \alpha_1 \mathbf{M} + \alpha_2 \mathbf{K} \quad (11.13)$$

is chosen. The coefficients are set to $\alpha_1 = 1$ and $\alpha_2 = 3 \times 10^{-4}$ which is similar to the damping observed in experiments. In the first parametric study the functionality of the PLL method for tracking of the backbone curve is illustrated. The structure is excited at the second node with a harmonic force and the displacement of the same node is also chosen as reference for the PLL tuning. Generally, the choice of the reference node is arbitrary as the NNM motion is assumed to be a monophase motion. However, this assumption does not necessarily hold in the damped and forced system as there might be a small phase difference between different DOFs. Additionally, the phase and amplitude of higher harmonics can have some influence on the phase of the reference signal in Eq. (11.6). To get started, it seems to be a natural choice to use the node of the excitation as reference. The system is modeled in Matlab/Simulink and time integration is used to study the closed loop behavior of the system including the PLL. The amplitude of the excitation force is incrementally increased as shown in Fig. 11.6 starting

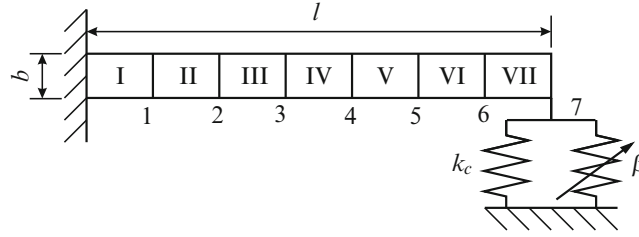


Fig. 11.4 Schematic sketch of the experimental beam

Table 11.1 Parameters of numerical beam structure

Parameter	Value	Unit
E	185	GPa
ρ	7830	kg/m ³
β	8×10^9	N/m ³
k_c	1000	N/m
l	700	mm
b	12	mm

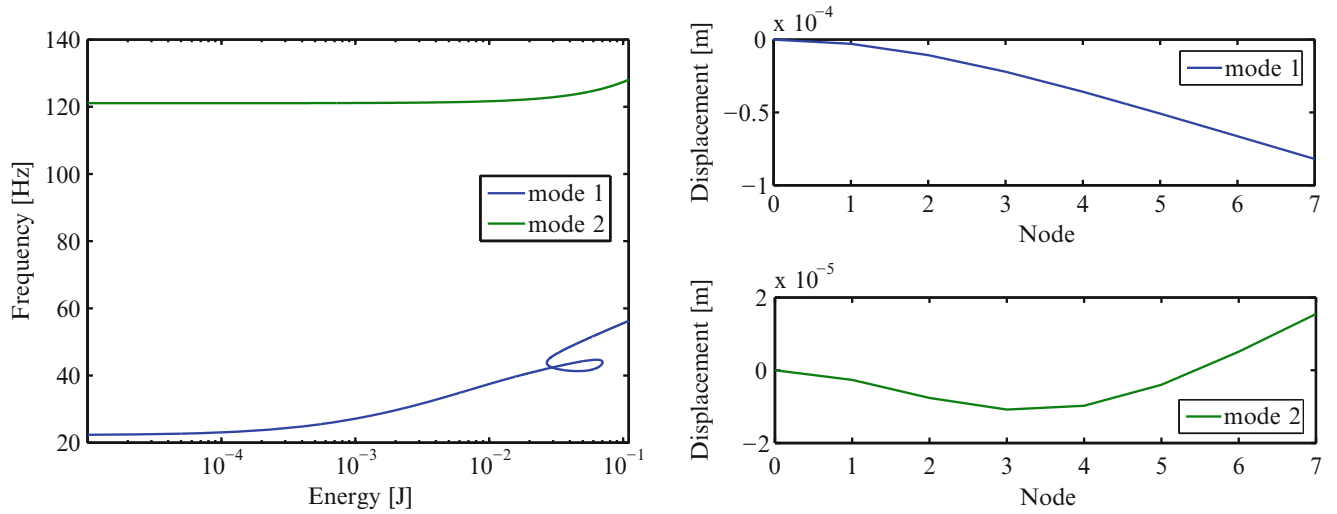


Fig. 11.5 Left: FEP of first two modes of the beam. Right: Mode shapes in linear range of the first two modes

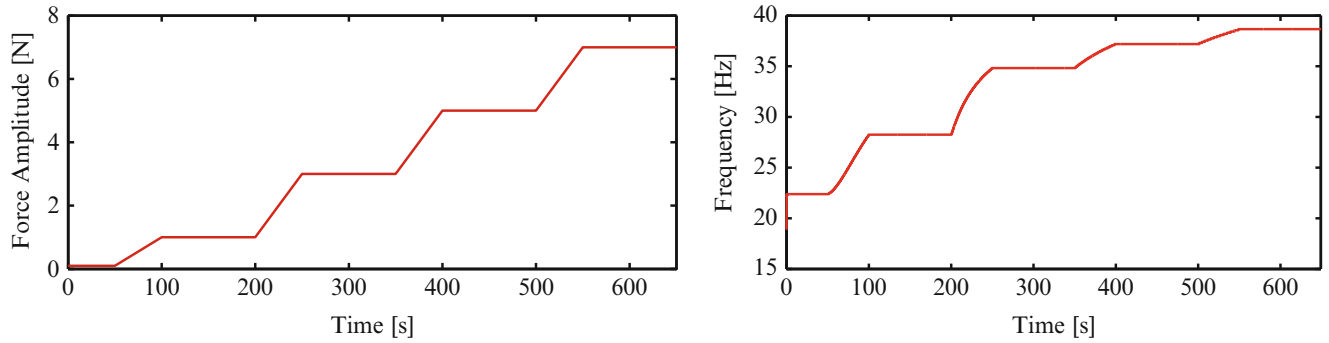


Fig. 11.6 Left: Amplitude of harmonic forcing. Right: Frequency of maximum wavelet coefficient of the force signal

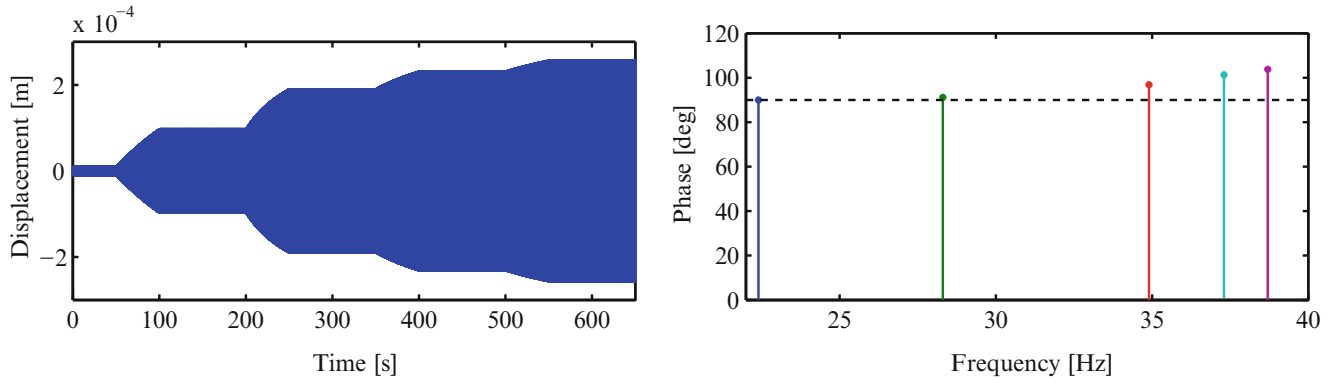


Fig. 11.7 Left: Time signal of the acceleration at the reference node. Right: Phase of first harmonic with respect to the forcing

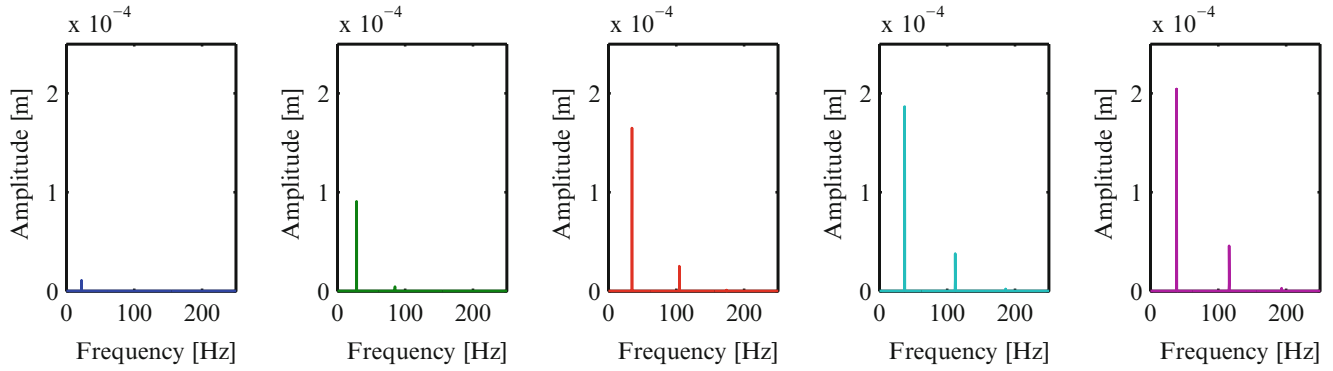


Fig. 11.8 Amplitude spectrum of response for increasing forcing amplitude $\hat{F}_{\text{exc}} = \{0.1, 1, 3, 5, 7\}$ N

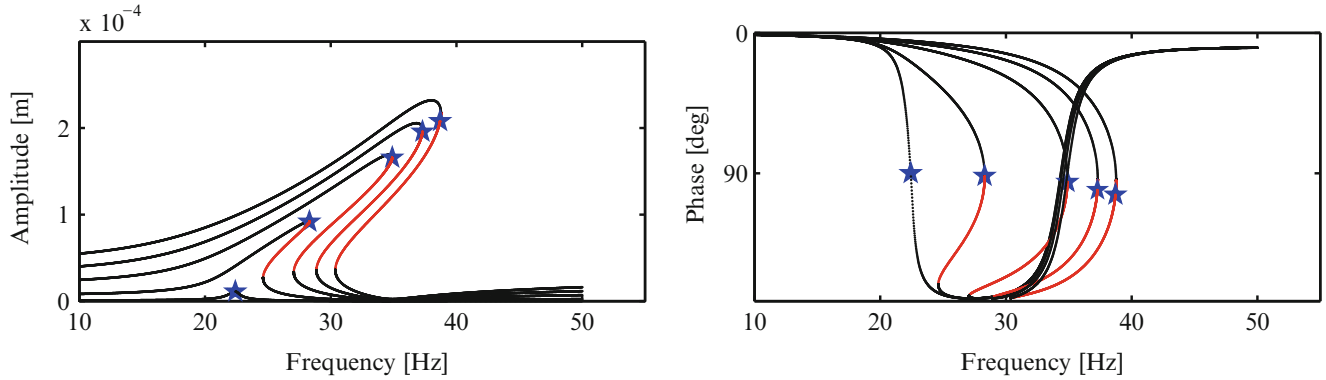


Fig. 11.9 Left: First harmonic FRF for system with harmonic excitation (black: stable; red: unstable). Right: Phase lag of first harmonic with respect to the forcing (black: stable; red: unstable)

from an initial value of 0.1 N, where the structure behaves almost linearly. The instantaneous frequency of the forcing which was extracted by the wavelet transform is plotted in Fig. 11.6. It can be observed that the linear eigenfrequency is found quickly and the PLL reaches the locked state. By increasing the forcing level up to 7 N the resonance frequency is shifted and the PLL tunes the excitation frequency.

The displacement at the reference node is displayed in Fig. 11.7. For the analysis of the results, this displacement is transformed into the frequency domain using an FFT such that the amplitudes (Fig. 11.8) and phases (Fig. 11.7) can be compared to the calculated FRFs of the system (Fig. 11.9). The FRFs are calculated using the HBM taking into account five harmonics and the stability of the FRF is determined using Hill's method [29].

In comparison, the amplitude and frequency of the first harmonic of the time signal obtained by the PLL is in very good agreement with the first harmonic of the FRF. The same also holds for higher harmonics which are not studied in a more detailed way at this point. However, an interesting aspect of the PLL testing can be observed regarding the phase lag of the

first harmonic with respect to the force. For low level excitation the phase lag is maintained at exactly 90° but for increasing excitation levels there is an increasing deviation. This effect is caused by the increase of the third harmonic, which is not in phase with the fundamental harmonic if only an imperfect force appropriation is applied. The phase detector basically relies on the first harmonic of the reference signal. As the sign detection in Eq. (11.4) is used to generate the reference signal, the phase of its first harmonic is shifted if the displacement signal contains higher harmonics with a shifted phase with respect to the fundamental. Still, this effect plays a minor role especially as the appropriate excitation is approximated by a single harmonic single point force, anyway. In the present example this can be observed when the system is driven close to the 1:3 internal resonance, where the third harmonic is amplified by the second mode. Another interesting aspect of the PLL method can herein be observed regarding the stability calculations of the FRF in Fig. 11.9. The points in which the system is driven by the PLL controller are marked with the blue star in the FRF and phase response. It can be seen that due to the small phase deviation induced by higher harmonics the PLL drives the system in a region which is unstable in the FRF. This illustrates the stabilizing effect of the close loop on the system that also helps to drive the system near jumps without facing the problem of premature jumping.

11.4.1 Effect of Internal Resonance on PLL Measurements

In the FEP it was observed that the parameters of the beam are chosen in a way that a 1:3 internal resonance can strongly affect the system's behavior when the energy exceeds a certain level. Once the system is excited at a certain level the third harmonic becomes strongly amplified by the second mode. As previously shown the strong third harmonic component may lead to a small shift in the detected phase, which depends on the amplitude and the phase of the third harmonic component relative to the fundamental. To study this effect, the forcing amplitude is increased further as it is shown in Fig. 11.10 and the robustness of the PLL method is investigated. The FRF in Fig. 11.10 shows that due to the internal resonance the amplitude of the third harmonic can be up to one third of the fundamental harmonic. The tests with the PLL method show that nevertheless the phase, frequency and amplitude errors remain small. For illustration, the test results for this specific test case are shown in Figs. 11.11 and 11.12 respectively.

It is also interesting to observe that for the highest forcing the region of the internal resonance is already passed, which results in a vanishing phase deviation. Generally, it was observed that the method is very robust even in the presence of strong higher harmonics. Even though there is some inaccuracy in the region of the internal resonance the PLL is capable of keeping track of the NNM branch. For motions which are dominated by a higher mode due to an internal resonance, first numerical experiments showed that the PLL can lock to the higher mode and tune the excitation frequency based on this mode. In this context the choice of the reference node seems to be an interesting factor, as at different points of the structure different modes can be measured. A more detailed discussion of these cases is beyond the scope of this paper since these effects were also not observed in the subsequent experimental test.

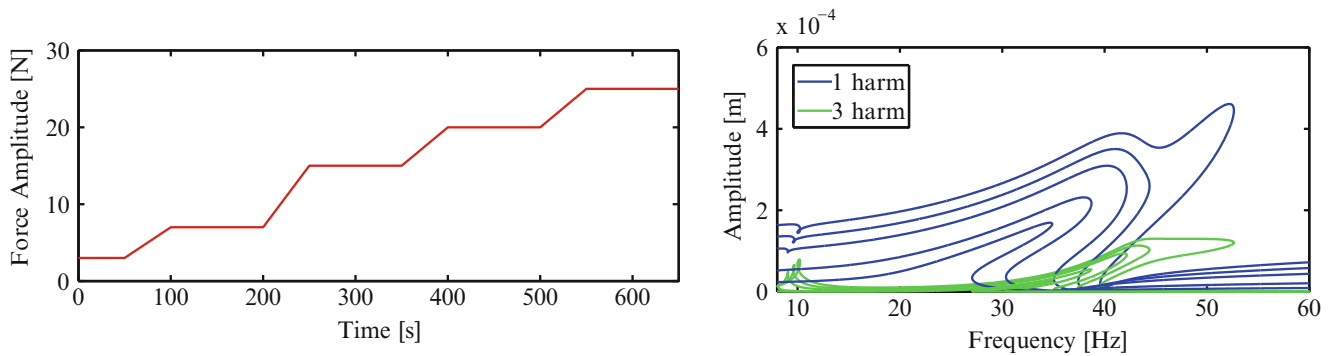


Fig. 11.10 Left: Amplitude of harmonic forcing. Right: First and third harmonic FRF at reference node

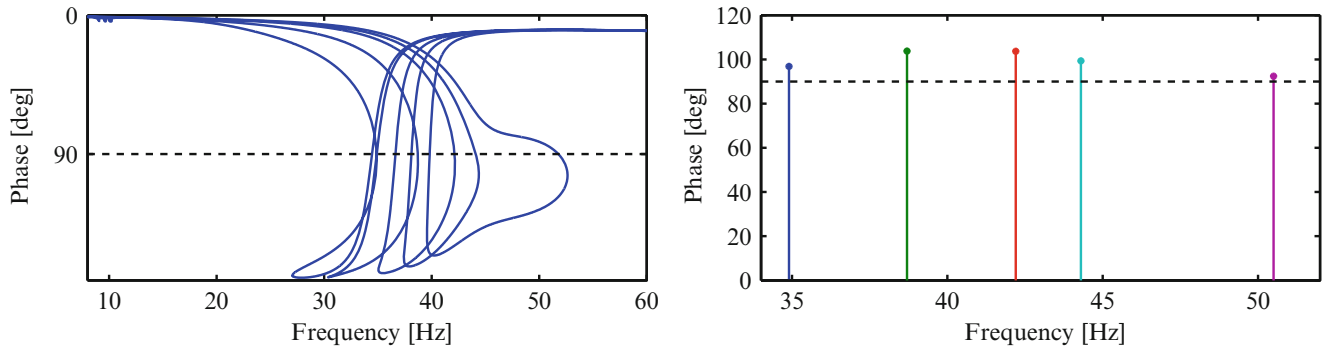


Fig. 11.11 Left: Phase first harmonic of calculated FRF. Right: Phase of first harmonic of PLL test

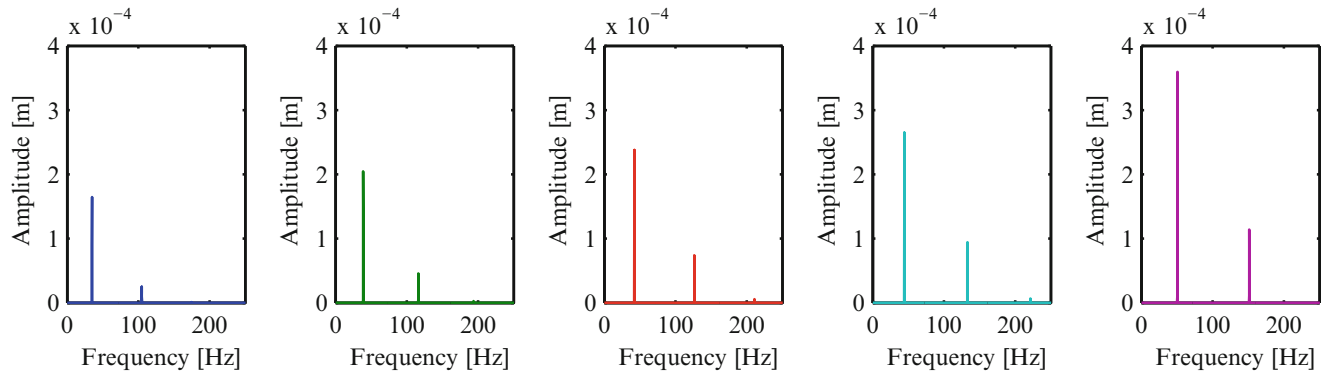


Fig. 11.12 Amplitude spectrum of response for increasing forcing amplitude $\hat{F}_{\text{exc}} = \{3, 7, 15, 20, 25\}$ N

11.5 Experimental Demonstration for a Beam with Cubic Nonlinearities

The experimental setup is similar to the numerical example in the previous section with some different parameters. It consists of a clamped steel beam with a thin beam at the tip which is also clamped. The clamping of the thin beam can be moved by an adjusting screw and the pretension of the specimen can be measured with a strain gauge located on the thick beam. Due to the clamped-clamped setup of the beam structure a geometric nonlinearity can be observed in the case of large deflection. A photo of the setup is displayed in Fig. 11.13 and a schematic sketch where the small beam and its nonlinearity is represented by a three parameter model is shown in Fig. 11.14.

The parameters for the beam without pretension, that were obtained through a model updating procedure based on the NNMs of the system which was presented in a previous publication [30], are listed in Table 11.2. The differences compared to the numerical example mainly have two consequences. Firstly, the 1:3 internal resonance is not observed in the practical experiment as even for the setup without pretension the first eigenfrequency is higher than one third of the second one. For this setup the FRF in the linear range is shown in Fig. 11.15. The higher resonance frequencies that appear in the FRF also do not lead to significant internal resonances. Secondly, the adjustment of the pretension in the beam shifts the linear eigenfrequencies as it can be seen in Fig. 11.15. It can be observed that the first eigenfrequency is affected most by an increasing pretension, which means that also for higher pretension no 1:3 internal resonance will play a role.

The PLL is implemented on a DSPACE rapid prototyping system and the force is measured with a load cell at the point of the shaker excitation. The reference signal for the PLL is obtained based on accelerometer measurements. In the first experimental test, a parametric study for the detection of the linear resonance frequency using the PLL is carried out. Therefore, the beam without pretension is excited on the second node with a small excitation amplitude of 0.5 N and the effect of different center frequencies of the VCO is investigated. The second node was also used as reference for the phase criterion. The wavelet transform was used to extract the instantaneous frequency of the excitation force over time. This frequency is plotted for the different center frequencies in Fig. 11.16. It can be observed that the VCO starts oscillating at its center frequency and therefore generates a harmonic force signal with this frequency at the very beginning of the measurement. Then the frequency changes until the PLL is in a locked state, generating a steady state harmonic signal with a certain frequency. For the first five center frequencies, the PLL locks to the first eigenfrequency even for starting frequencies

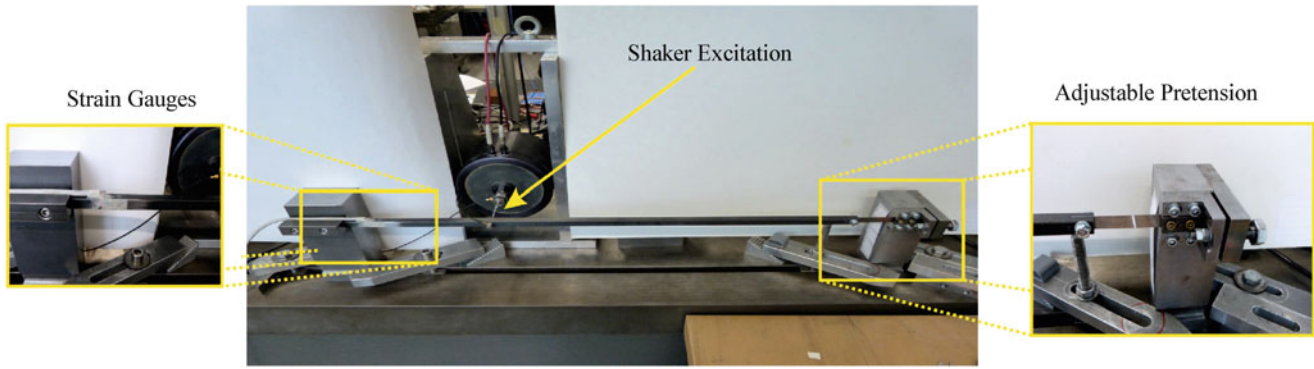


Fig. 11.13 Experimental setup of the benchmark beam

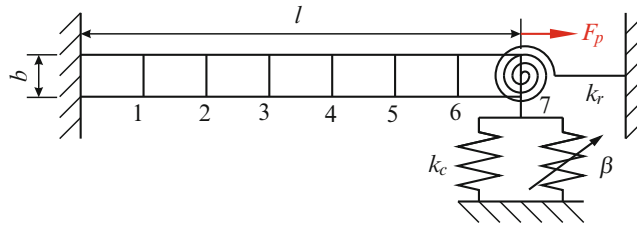


Fig. 11.14 Schematic sketch of the experimental beam

Table 11.2 Parameters of beam without pretension

Parameter	Value	Unit
E	186	GPa
k_c	5525	N/m
k_r	217	Nm/rad
β	203×10^6	N/m ³
l	700	mm
b	12	mm

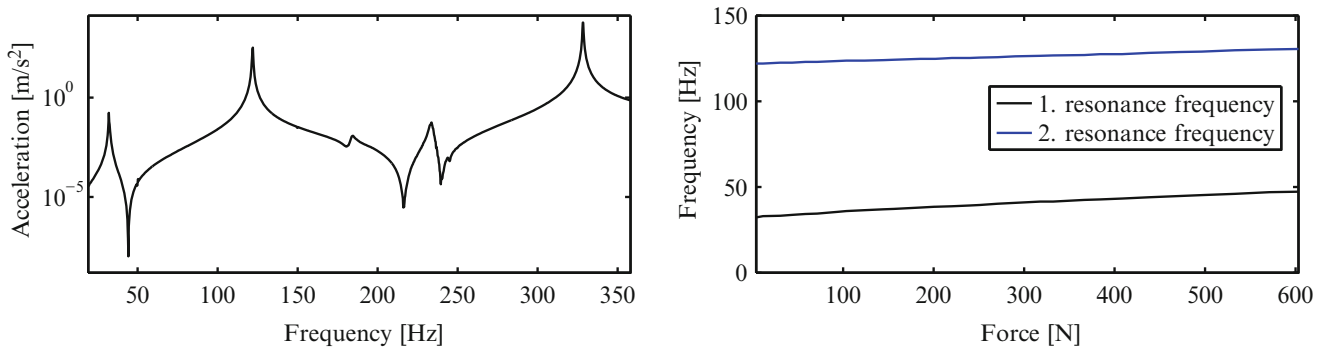


Fig. 11.15 Left: FRF for beam without pretension. Right: Resonance frequencies of the beam dependent on pretension

which are up to 70 % off the actual eigenfrequency. It can also be seen that the detection of the eigenfrequency works for an initial center frequency which is higher or lower than the eigenfrequency. However, if the initial frequency is too high, the motion is dominated by the second mode and the PLL locks to this mode as can be observed in the last figure. The parametric study clearly shows that the center frequency of the VCO is uncritical for the detection of the modes such that no a priori knowledge of the linear eigenfrequencies is required.

After detection of the linear eigenfrequency, the excitation amplitude is incrementally increased and the capability of the PLL to track the backbone curve in the nonlinear range is investigated. For this test, the pretension is increased to 300 N,

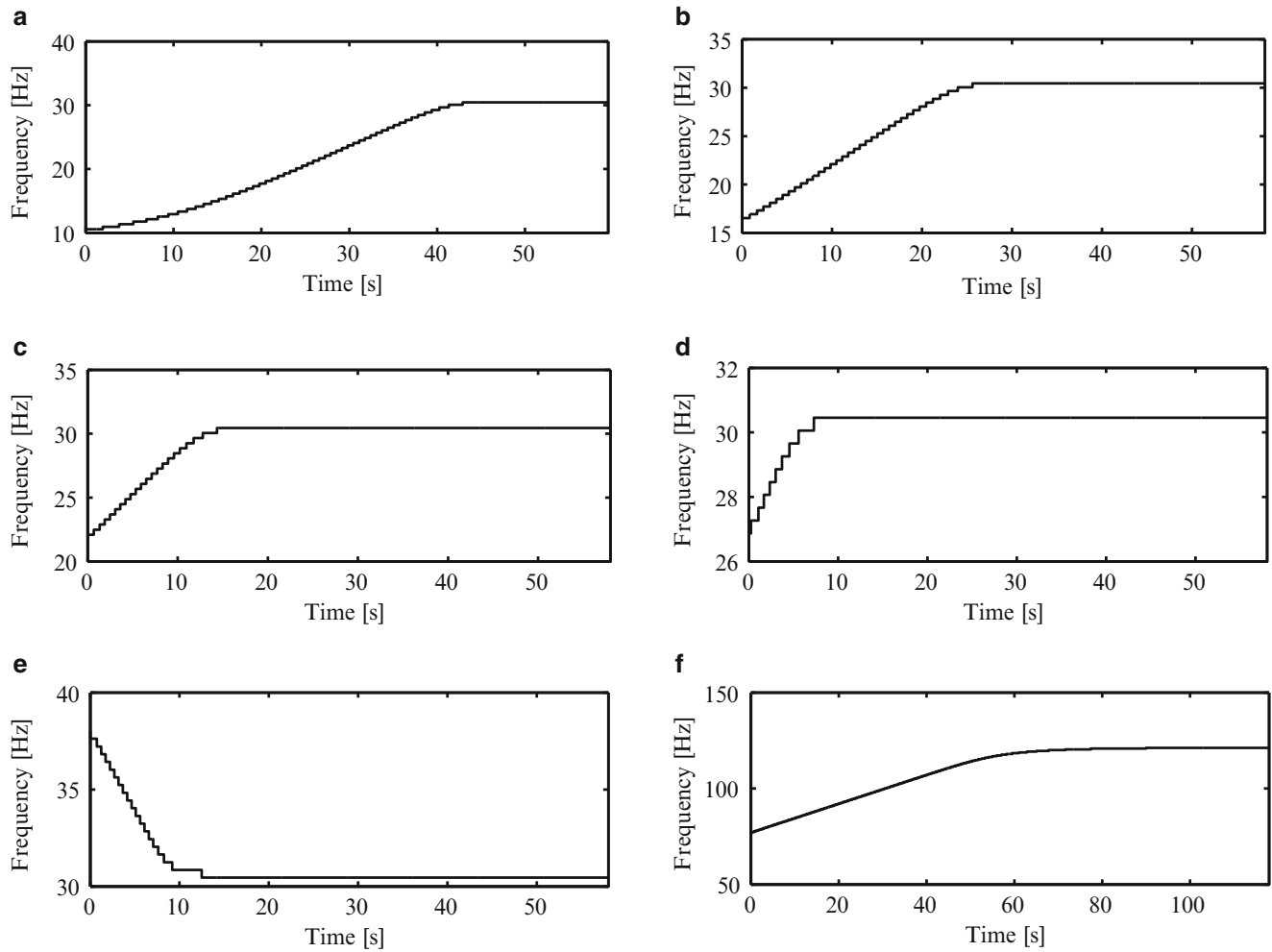


Fig. 11.16 Frequency with maximum forcing amplitude for different VCO center frequencies $f_c = \{10, 15, 20, 25, 37, 75\}$ Hz

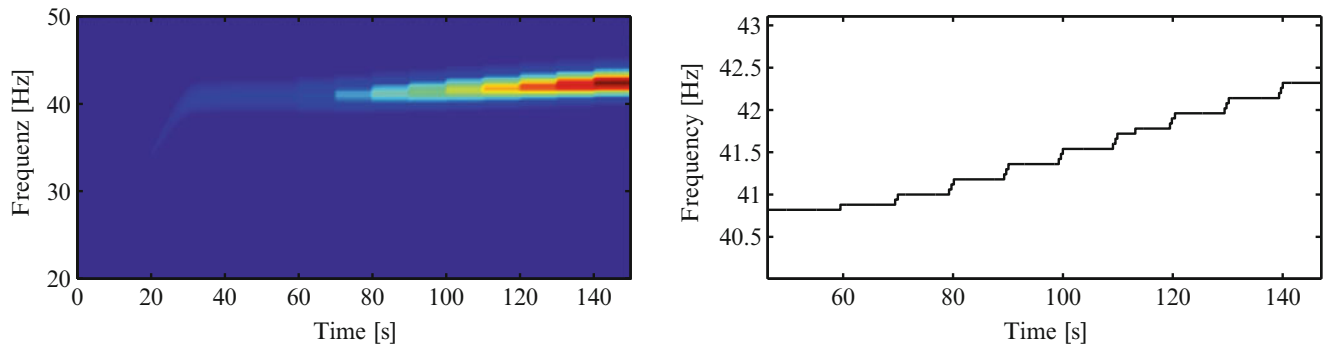


Fig. 11.17 *Left:* Wavelet transform of the acceleration signal. *Right:* Frequency of the maximum wavelet coefficient

leading to a linear eigenfrequency of 40.8 Hz. Especially for longer experiments with high deflection, the temperature in the small beam increases, which can lead an expansion and therefore to buckling in the small beam resulting in dramatic changes in the behavior of the setup. The pretension in the beam helps to avoid this phenomenon and enhances the repeatability of the measurements. For the tracking of the backbone curve in the nonlinear range, the forcing amplitude is increased from 1 to 10 N in steps of 1 N. The forcing is held constant for 60 s during the initial detection of the linear eigenfrequency. When the PLL is in the locked state in the linear eigenfrequency the forcing is increased after intervals of 10 s. The wavelet transform of the acceleration signal is shown in Fig. 11.17.

It can be observed that with each increment of the forcing, the amplitude and therefore the wavelet coefficient increases. Due to the stiffening behavior of the system the resonance frequency increases with higher amplitude such that the maximum of the wavelet transform is shifted to higher frequencies. The PLL automatically adjusts the frequency of the forcing to maintain the resonance criterion to be fulfilled. In laboratory experiments, the testing with the PLL turns out to be very user-friendly, as during the testing no manual action is necessary. Furthermore, the incremental increase of the forcing from low level to high level in resonance does not require any a priori knowledge of maximum forcing amplitude. The test can automatically be stopped once a maximum acceleration is exceeded and all previously recorded points of the backbone curve are retained.

11.6 Conclusion and Future Work

This paper presents a new method, simplifying phase resonance testing of nonlinear structures. A PLL controller is used to automatically maintain the phase criterion during the nonlinear modal test. The design of the PLL implemented for this purpose has briefly been discussed and the differences to classical phase resonance tests have been highlighted. The features of the proposed method have been studied in an extensive numerical example comparing NNM computations with the HBM with time integrations results of systems driven by the PLL controlled excitation force. It has been illustrated that the method is robust even in the presence of strong higher harmonics. The PLL is implemented in a real experimental setup and has successfully been demonstrated for an experimental benchmark structure with strong geometric nonlinearity. The new method provides several advantages compared to classical phase resonance testing. With the automated procedure, the energy dependent modes of nonlinear systems can be tracked in a fast and user-friendly way. No manual action during the testing is necessary reducing the chance of operator errors and improving the repeatability of the measurements. The testing from a low level to a high level excitation is beneficial for unknown structures. Additionally, the influence of transient effects can be eliminated as steady state measurements are used to identify the backbone curve. Due to the stabilizing effect of the PLL small phase inaccuracies do not affect the robustness of the method and the frequency amplitude relation can be extracted accurately. The method proved its robustness even in the case of an internal resonance amplifying higher harmonics.

In future research the PLL method will be applied to more complex structure with different nonlinearities. The behavior of the method in regions of internal resonances will be studied in a more detailed way. Additionally experimental studies with systems exhibiting internal resonances will be carried out and the effect of inaccuracies in the appropriate excitation is investigated. In this context, it will also be interesting to take the shaker-structure interaction into account, which naturally leads to higher harmonics in the forcing function. The extension to non-conservative systems, e.g. using the concept of complex nonlinear modes will be another future challenge.

References

1. Rosenberg, R.M.: Normal modes of nonlinear dual-mode systems. *J. Appl. Mech.* **27**, 263–268 (1960)
2. Shaw, S.W., Pierre, C.: Normal modes for non-linear vibratory systems. *J. Sound Vib.* **164**, 85–124 (1993)
3. Vakakis, A.F., Manevitch, L.I., Mikhlin, Y.V., Pilipchuk, V.N., Zevin, A.A.: *Normal Modes and Localization in Nonlinear Systems*. Wiley, New York (1996)
4. Kerschen, G., Peeters, M., Golinval, J.-C., Vakakis, A.F.: Nonlinear normal modes, part I: a useful framework for the structural dynamicist. *Mech. Syst. Signal Process.* **23**, 170–194 (2009)
5. Kerschen, G., Peeters, M., Golinval, J.-C., Stéphan, C.: Nonlinear modal analysis of a full-scale aircraft. *J. Aircr.* **50**, 1409–1419 (2013)
6. Detroux, T., Renson, L., Kerschen, G.: The harmonic balance method for advanced analysis and design of nonlinear mechanical systems. In: *Proceedings of the IMAC-XXXII, Orlando, FL* (2014)
7. Krack, M., Panning-von Scheidt, L., Wallaschek, J.: A method for nonlinear modal analysis and synthesis: application to harmonically forced and self-excited mechanical systems. *J. Sound Vib.* **332**, 6798–6814 (2013)
8. Kuether, R.J., Renson, L., Detroux, T., Grappasonni, C., Kerschen, G., Allen, M.S.: Prediction of isolated resonance curves using nonlinear normal modes. In: *Proceedings of ASME IDETC 2015, Boston, MA* (2015)
9. Peeters, M., Vigui, R., Srandour, G., Kerschen, G., Golinval, J.-C.: Nonlinear normal modes, part II: toward a practical computation using numerical continuation techniques. *Mech. Syst. Signal Process.* **23**, 195–216 (2009)
10. Laxalde, D., Thouverez, F.: Complex non-linear modal analysis for mechanical systems: application to turbomachinery bladings with friction interfaces. *J. Sound Vib.* **322**, 1009–1025 (2009)
11. Peeters, M., Kerschen, G., Golinval, J.C.: Dynamic testing of nonlinear vibrating structures using nonlinear normal modes. *J. Sound Vib.* **330**, 486–509 (2010)
12. Peeters, M., Kerschen, G., Golinval, J.C.: Modal testing using nonlinear normal modes: an experimental demonstration. In: *Proceedings of ISMA 2010, Leuven* (2010)

13. Londono, J.M., Cooper, J.E., Neild, S.A.: Vibration testing of large scale nonlinear structures. In: Proceedings of ISMA 2014, Leuven (2014)
14. Noël, J.P., Renson, L., Grappasonni, C., Kerschen, G.: A rigorous phase separation method for testing nonlinear structures. In: Proceedings of ISMA 2014, Leuven (2014)
15. Staszewski, W.J.: Identification of non-linear systems using multi-scale ridges and skeletons of the wavelet transform. *J. Sound Vib.* **214**, 639–658 (1998)
16. de Bellescize, H.: La réception synchrone. *L'Onde Électrique* **11**, 230–240 (1932)
17. Best, R.E.: Phase-Locked Loops - Design, Simulation and Applications, 6th edn. McGraw Hill, New York (2007)
18. Abramovitch, D.Y.: Phase-locked loops: a control centric tutorial. In: Proceedings of the American Control Conference, Anchorage, AK (2002)
19. Hsieh, G.-C., Hung, J.C.: Phase-locked loop techniques - a survey. *IEEE Trans. Ind. Electron.* **43**(6), 609–615 (1996)
20. Fan, M., Clark, M., Feng, Z.C.: Implementation and stability study of phase-locked-loop nonlinear dynamic measurement systems. *Commun. Nonlinear Sci. Numer. Simul.* **12**, 1302–1315 (2007)
21. Sun, X., Horowitz, R., Komvopoulos, K.: Stability and resolution analysis of a phase-locked loop natural frequency tracking system for MEMS fatigue testing. *J. Dyn. Syst. Meas. Control* **124**, 599–605 (2002)
22. Mojrzisch, S., Ille, I., Wallascheck, J.: Phase controlled frequency response measurement for nonlinear vibration systems. In: Proceedings of ICSV 2013, Bangkok (2013)
23. Peter, S., Schreyer, F., Reuss, P., Gaul, L.: Consideration of local stiffening and clearance nonlinearities in coupled systems using a generalized harmonic balance method. In: Proceedings of ISMA 2014, Leuven (2014)
24. Gasch, R., Knothe, K., Liebich, R.: *Strukturdynamik*. Springer, Berlin (2012)
25. Gardner, F.M.: *Phaselock Techniques*. Wiley, New York (2005)
26. Lunze, J.: *Systemtheoretische Grundlagen, Analyse und Entwurf einschleifiger Regelungen*. Springer, Berlin (2014)
27. Abramovitch, D.Y.: Lyapunov redesign of analog phase-lock loops. *IEEE Trans. Commun.* **38**(12), 2197–2202 (2002)
28. Thouverez, F.: Presentation of the ECL benchmark. *Mech. Syst. Signal Process.* **17**, 195–202 (2003)
29. Lazarus, A., Thomas, O.: A harmonic-based method for computing the stability of periodic solutions of dynamical systems. *C. R. Méc.* **338**, 510–517 (2010)
30. Peter, S., Grundler, A., Reuss, P., Gaul, L., Leine, R.I.: Towards finite element model updating based on nonlinear normal modes. In: Proceedings of the IMAC-XXXIII, Orlando, FL (2015)